NiNbO Catalyst Deposited on Anodized Aluminum Monoliths for the Oxidative Dehydrogenation of Ethane

José A. Santander,* Diego E. Boldrini, Marisa N. Pedernera and Gabriela M. Tonetto

Planta Piloto de Ingeniería Química PLAPIQUI (UNS – CONICET), Camino "La Carrindanga" Km 7, CC 717, CP 8000, Bahía Blanca, Argentina

Aluminum monoliths were used as substrates to prepare structured catalysts. A rough alumina layer was generated on the surface of the substrates by anodizing followed by hydrothermal treatments. The dip-coating technique was used for coating the monolithic substrates. Aqueous suspensions with 0.15 and 0.30 g/g of Ni-Nb mixed oxides catalysts were prepared for that purpose. Colloidal SiO_2 was added as a binder in order to obtain homogeneous and adherent coatings. The samples were characterized by SEM, TPR, XPS, XRD, and N_2 adsorption and tested in the oxidative dehydrogenation (ODH) of ethane to ethylene. The silica particles produced a drop in catalytic activity without affecting ethylene selectivity. The former effect was attributed mainly to a decrease in surface nickel concentration and an increase in reduction temperature. The presence of anodized aluminum substrates in the reaction environment did not have a significant influence on catalytic activity and product distribution, as observed for the coated monoliths used in this work, thus being a useful material to prepare structured catalysts for low-temperature ethane ODH.

Keywords: heterogeneous catalysis, structured reactors, partial oxidation, nickel, niobium

INTRODUCTION

Ethylene is a building block for the chemical industry and is the most important basic petrochemical product for making plastics, ethylene oxides, and other chemicals.[1] Twenty-one percent (21 %) of ethylene is produced by steam cracking of ethane, and the rest is mainly produced by thermal cracking of petrochemical feedstocks such as naphtha, propane, and gas oil.[2] A promising route for ethylene production is the catalytic conversion of ethane under oxidizing conditions: the oxidative dehydrogenation (ODH) of ethane. This route presents advantages over steam cracking, such as lower reaction temperatures and the absence of thermodynamic equilibrium limitations. However, catalytic ethane ODH is exothermic so that the control of the reaction temperature appears as a key factor to maintain a good selectivity level. In this sense oxydehydrogenation of ethane to ethylene could be efficiently conducted in structured reactors.[3–5] Monolithic catalysts offer a number of advantages over conventional packed beds, mainly associated with reduction in pressure drop, mechanical integrity, improved heat transfer, and reduced size.[6]

Typical support materials of monoliths are ceramics and metals. Metallic structures present several advantages over ceramic monoliths in terms of enhanced thermal conductivity and higher mechanical resistance. They also exhibit a greater flexibility in the design and the possibility of using thinner walls leading to higher cell density and lower pressure drop.[7,8] An important issue in the use of metallic substrates is the fixation of the catalyst layer, since flat metal surfaces lead to a low adherence of the coating. When the deposition of the catalytic material is performed using techniques such as dip-coating (immersion of the substrate into a slurry of catalyst particles), an effective route for improving adhesion is to incorporate additives that promote the mechanical anchorage of the catalyst to the substrate surface. In the present contribution, colloidal silica was used as an inorganic binder to enhance the coating adherence, and the effects of this additive on the catalytic properties of the system are particularly reported. Nevertheless, pre-treatment of the substrate is usually required in order to increase surface roughness, thus promoting the fixation of the catalyst. For medium-low temperature processes, as in the oxidative dehydrogenation over Ni-based catalysts, aluminum is an adequate structural material to prepare metallic monoliths. Aluminum coated with alumina produced by anodization is an excellent material to prepare metallic monoliths. The anodizing process generates an alumina coating that is highly adherent, stable, and capable of having its textural properties adjusted by modifying the anodizing parameters to enhance the catalytic material anchoring.[9,10] Hydrothermal treatments are an alternative way to modify alumina surface morphology, increasing the surface area and changing the pore structure.[11,12]

The use of anodized aluminum as structured substrate in gas-phase oxidation reactions was previously reported.[13–16] Lee and Gavriilidis[13] prepared $Au/Al_2O_3/Al$ thin film catalysts by impregnation of anodized aluminum plates for low-temperature CO oxidation. Sanz et al.[14] prepared anodized aluminum monoliths as support for $Au\text{-}CeO_2$ catalysts. Under extreme anodization process conditions (30 °C, 50 min, 2 $A \cdot dm^{-2}$, and 2.6 mol/L of sulphuric acid), significant cracks were obtained and used to fix the catalytic coatings. The resulting monolithic catalysts were also tested in the CO oxidation reaction, higher Au concentration catalysts being the most active. For oxidative dehydrogenation reactions, Feng et al.[16] prepared a nanoporous anodic aluminum oxide (AAO) structure in the centre of an aluminum disc, coating the nanopore walls with catalytically active materials so that the structure functioned as an array of

* *Author to whom correspondence may be addressed.*
E-mail address: jsantander@plapiqui.edu.ar
Can. J. Chem. Eng. 9999:1–9, 2017

DOI 10.1002/cjce.22800
Published online in Wiley Online Library (wileyonlinelibrary.com).

tubular reactors. The structured catalyst was tested for ODH of cyclohexane, the monolithic system being superior to a conventional powder catalyst in terms of selectivity to the partial oxidation product.

One of the most important catalytic systems for ODH of ethane is NiO-based catalysts.[17–20] Unpromoted NiO is an active but nonselective catalyst for the ODH of ethane. Doping nickel oxide with high valence cations[21] increases ethylene selectivity due to the reduction of the nonstoichiometric oxygen, which in high concentration promotes total oxidation reactions. Ni-Nb mixed oxides prepared with a Nb:Ni atomic ratio of 0.176 exhibit high activity and selectivity at low temperatures, with ethylene yields above 40 % at 400 °C.[17,22–24]

In this paper, the coating of anodized aluminum monoliths with selective Ni-Nb oxides catalysts by dip-coating technique is reported. The influence of suspension composition on the homogeneity and integrity of the catalytic layer was studied. The monolithic catalysts were tested in the oxidative dehydrogenation of ethane, and the effect of inorganic binders in the activity and ethylene selectivity was analyzed.

EXPERIMENTAL

Preparation of the Powder Catalyst

The Ni-Nb mixed oxide powder catalyst was obtained by the evaporation method. The selected Nb:Ni atomic ratio of 0.176 was reported to be optimum for ethane ODH reaction.[17] First, an aqueous solution of nickel(II) nitrate hexahydrate (Tetrahedron, 98 %) and ammonium niobate-(V) oxalate hydrate (Aldrich, 99.99 %) was prepared. Then the solvent was evaporated at 70 °C under continuous agitation and dried at 120 °C for 12 h. The resulting material was calcined at 450 °C for 5 h. The powder catalyst obtained presented a particle size $d_{90} = 3.04 \times 10^{-6}$ m and was denoted as NiNbO.

Preparation of Structured Substrates

Anodized aluminum monoliths were prepared using commercial laminated pure aluminum sheets as metallic substrate (Aluar A1050). The anodizing technology was used to generate an alumina layer on the surface of the 0.1 mm thick aluminum sheets in order to increase the roughness of the substrate.[25] The operating conditions for the anodizing process were: electrolyte: oxalic acid (Aldrich, 98 %), electrolyte concentration: 1.6 mol/L, temperature: 40 °C, current density: 2 $A \cdot dm^{-2}$, time: 40 min anodizing + 40 min pore opening.

After anodizing, the metal sheets were washed and dried (60 °C for 30 min). Al_2O_3/Al monoliths were prepared by rolling previously-anodized flat and corrugated foils around a spindle. The final monolith was a cylinder of 15 mm diameter by 15 mm height and a cell density of 54 cells per square centimeter. The main physical characteristics of the anodized aluminum monoliths are given in Table 1.

The monoliths were exposed to the following treatments.[11] First, a thermal treatment was performed in order to remove traces of oxalic acid remaining in the pores and to stabilize the formed alumina (pretreatment denoted as T1). The oven temperature was raised from room temperature to 500 °C at a heating rate of 2 °C · min^{-1} and it was held at 500 °C for 2 h in flowing air (Air Liquide, 99.999 %). Then the aluminum foils were hydrothermally treated by immersion in deionized water at 100 °C for 1 h and dried in a convection oven at 60 °C for 60 min and 150 °C for 30 min (treatment H1). Finally, the alumina dehydration was accomplished by heating to 500 °C in a tube furnace under flowing air for 16 h (treatment T2).

Preparation of the Structured Catalysts

The monolithic substrates were coated with the catalyst by the dip-coating technique. For that purpose, aqueous suspensions with 0.15 and 0.30 g/g of Ni-Nb mixed oxide catalysts were prepared.[26] In all cases, 0.10 g/g colloidal SiO_2 (Ludox TMA, Aldrich) was added as a binder. In some suspensions, 0.02–0.03 g/g of polyvinyl alcohol (PVA) was added to control the drying rate. Part of the 0.30 g/g catalyst suspension that was not used in the coating was dried and calcined to obtain a powder with a particle size $d_{90} = 3.56 \times 10^{-6}$ m, denoted as CS-30. The aluminum monoliths were dipped and withdrawn from the suspensions, the excess material being removed by centrifugation at 500 rpm for 3 min. Then the substrates were dried at 80 °C for 30 min. The procedure was repeated until the desired catalyst loading of 180–280 mg was obtained. Finally, the samples were calcined at 400 °C for 2 h in air. The monoliths were labelled according to the catalyst loading used in the suspension. Catalytic monoliths prepared with 0.15 and 0.30 g/g catalyst suspensions were denoted as MA15 and MA30, respectively, whereas the sample prepared with the suspension containing 0.30 g/g catalyst and no addition of polyvinyl alcohol was named MA30noPVA.

Catalyst Characterization

The morphology of the substrate surface was examined by scanning electron microscopy (SEM) on a JEOL JSM 35CF microscope.

Temperature-programmed reduction (TPR) was carried out in a conventional apparatus equipped with a thermal conductivity detector. A detailed description of the equipment and the experimental conditions can be found elsewhere.[27]

The adherence of the catalytic layer deposited over the metallic substrates was tested by the ultrasonic method. The monoliths were immersed in 30 mL of diethyl ether and subjected to an ultrasonic bath for 30 min in a Cole Parmer 8892E-MT (47 kHz, 105 W) instrument at room temperature. Then, the solvent was evaporated. The weight of each monolith was measured before and after the ultrasonic treatment to determine the adherence, which was calculated as the percentage ratio of the amount of coating material retained to the amount of coating material present before the treatment.

Specific surface areas were determined by N_2 adsorption at 77 K, using the multipoint Brunauer-Emmett-Teller (BET) analysis method with a Quantachrome NOVA 1200e apparatus.

The amount of alumina generated during anodizing was determined by gravimetry. It was calculated from the weight difference of the anodized sheet before and after the chemical treatment which selectively dissolved the alumina layer. The dissolution process was carried out at 265 °C for 20 min using a 0.5 mol/L phosphoric acid and 0.2 mol/L chromic acid solution.

Table 1. Physical characteristics of the prepared aluminum monoliths

Parameter	
Monolith diameter (mm)	15
Channel length (mm)	15
Wall thickness (mm)	0.1
Monolith geometrical area (cm^2)	85
Cell density (cells · cm^{-2})	54
Surface area ($m^2 \cdot g_{monolith}^{-1}$)	40.7

X-ray diffraction (XRD) patterns were obtained using a Philips PW1710 diffractometer, with a monochromatic Cu-Kα source operating at 45 kV and 30 mA.

The X-ray photoelectron spectroscopy (XPS) measurements were conducted using a SPECS multi-technique system equipped with a dual Mg/Al X-ray source and a hemispherical PHOIBOS 150 analyzer operating in the fixed analyzer transmission (FAT) mode. The spectra were obtained with pass energy of 4806×10^{-18} J (30 eV), and the Mg Kα X-ray source was operated at 100 W.

Catalytic Tests

ODH of ethane was performed using a stainless steel tube of 16-mm inner diameter and 70-mm length where the monoliths were placed. The powder catalysts were tested in a fixed-bed reactor using a 4.2-mm inner-diameter glass tube. In the reactor, temperature measurements were carried out with a K thermocouple placed at the end of the catalytic bed or monolith. The experiments were carried out at atmospheric pressure and a reaction temperature range of 300–400 °C. The feedstock consisted of an $O_2/C_2H_6/N_2$ mixture with a 5/5/90 molar ratio. In all cases, the reactant flow rate was adjusted considering the amount of active phase (NiNbO) deposited on the monoliths and contained in the calcined suspension CS-30, maintaining an equal W:F ratio of 0.54 $g \cdot s \cdot cm^{-3}$. The amount of powdered catalyst used in the fixed bed reactor was 180–220 mg. The reaction products were analyzed with an HP Agilent 4890D gas chromatograph equipped with a thermal conductivity detector. Two columns were used in the analysis: Porapak QS and Molecular Sieve 0.5 nm.

The conversion of ethane was calculated using the following equation:

$$X_{C2H6}\ \% = \frac{2 \times F^{in}_{C2H6} - 2 \times F^{out}_{C2H6}}{2 \times F^{in}_{C2H6}} \times 100 \quad (1)$$

where F^{in}_{C2H6} and F^{out}_{C2H6} are the inlet and outlet molar flow rates of ethane in the reactor, respectively. The gas phase products selectivity was calculated according to the following:

$$S_i\ (\%) = \frac{n_i F_i}{\sum n_i F_i} \times 100 \quad (2)$$

where F_i refers to the molar flow rates of the reaction products and n_i to the number of carbon atoms in each chemical specie.

The ethylene yield was obtained by means of the following:

$$Y_{C2H4}\ (\%) = \frac{X_{C2H6}\ (\%) \times S_{C2H4}\ (\%)}{100} \quad (3)$$

In order to assess the experimental uncertainty between different reaction experiments, the experimental error was calculated by repeating a reaction test under identical conditions and using the same catalyst. In each test, the ethane conversion was evaluated at different temperatures with a constant pressure and reactants flow rate. Percent difference equation was used to compare the uncertainty of the measured conversions values at a specific temperature:

$$\text{Percent difference} = \frac{|E_1 - E_2|}{\frac{(E_1+E_2)}{2}} \times 100\ \%$$

where E_1 and E_2 are the conversion levels in experiments #1 and #2 at a particular temperature.

RESULTS AND DISCUSSION

Preparation of the Structured Substrates

The anodizing process conducted over the aluminum foils leads to the formation of an oxide layer strongly adhered to the substrate, presenting unbranched and regular pores. Figure 1 shows SEM micrographs of the anodized aluminum surface after the different

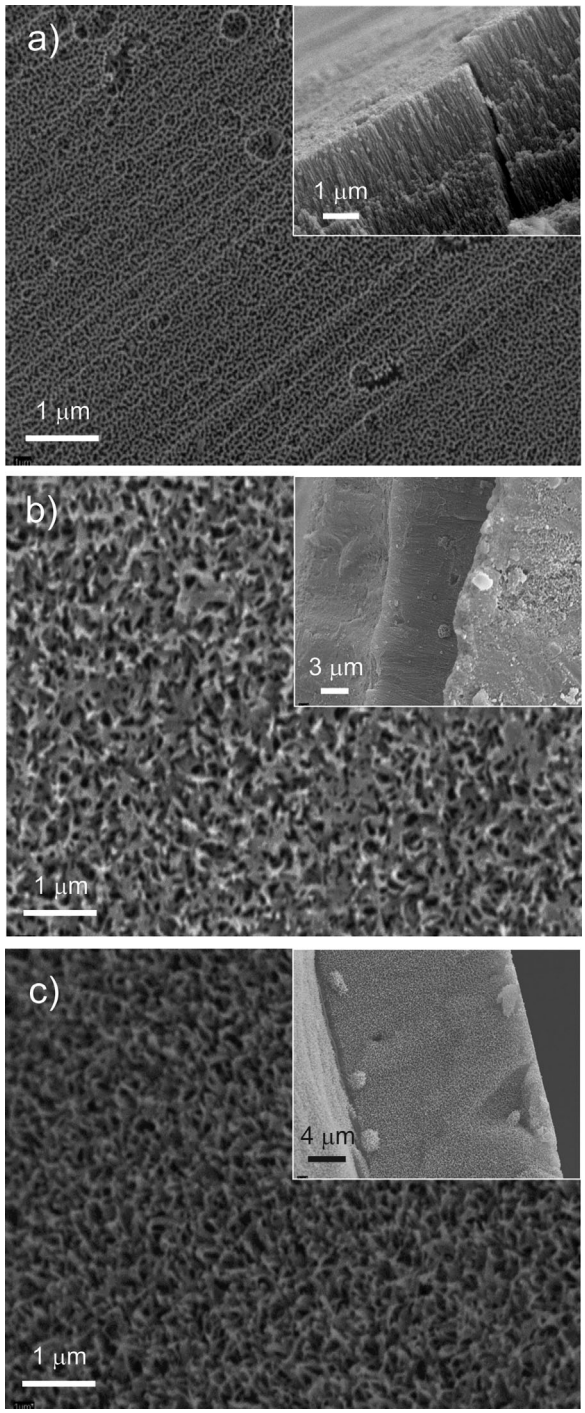

Figure 1. SEM micrographs of the anodized aluminum surface after the thermal-hydrothermal treatments. (a) Thermal treatment T1, (b) thermal-hydrothermal treatments T1-H1, and (c) thermal-hydrothermal treatments T1-H1-T2. The cross-sections of the alumina layers are shown in the corresponding insets.

Table 2. Textural properties of the Al_2O_3/Al monoliths after post-anodizing treatments

Post-anodizing treatments	Surface area ($m^2 \cdot g_{monolith}^{-1}$)	Pore radius (nm)	Pore volume ($cm^3 \cdot g^{-1}$)	Al_2O_3 thickness ($\times 10^6$ m)	Al_2O_3 generated ($g \cdot m^{-2}$)
T1	8.2	17.4	12×10^{-3}	17	34
T1-H1	48.2	1.87	52×10^{-3}	17	45
T1-H1-T2	40.7	1.87	46×10^{-3}	17	36

treatments, and the corresponding textural properties of the alumina layer are reported in Table 2. As shown in Figure 1a, after the anodizing and the first thermal treatment (T1) the amorphous alumina layer generated on the aluminum monolith was uniform and porous, with a thickness of approximately 17×10^{-6} m (Table 2). The entire surface was covered by regular pores (Figure 1a), with a mean pore radius of 17.4 nm. The textural properties of the alumina were significantly modified after the hydrothermal treatment (H1). The surface area was increased up to six times the original area and the pore structure of the anodic film was disintegrated. As observed in Figure 1b, the surface presented a cracked morphology, resulting in a rough surface that favours the mechanical anchorage of the catalytic material, enhancing its adherence to the substrate. The final thermal treatment (T2) resulted in the alumina dehydration with no significant modifications of the surface structure.

The thickness of the oxide layer remained constant after the three treatments (Table 2). However, an increase in the alumina mass was observed after treatment H1. When the hydrated oxides were calcined (T2), the original weight was recovered.

Preparation of the Structured Catalysts

The catalytic material was gradually deposited on the monoliths by successive immersions in the prepared suspensions until the catalyst loading was between 180–280 mg. The properties of the structured catalysts are shown in Table 3. As expected, the suspension with a lower concentration of solids led to a greater number of coating cycles (MA15 monolith) due to its lower slurry viscosity.[26] The samples with a higher amount of NiNbO catalyst (MA30 and MA30noPVA) required only a few immersions. For all samples, the amount of catalytic material increased linearly over the coating steps. The properties of the structured catalysts are shown in Table 3.

An excellent coating adherence was obtained for MA15 (99 %), attributed mainly to the higher silica:catalyst ratio in the deposited layer. During the drying process, the small silica particles are deposited at the interface between the larger catalyst particles by capillary forces, increasing the interaction between them.[28] Silica acts as a binder and improves the adhesion of the catalyst particles to the surface of the substrate, enhancing the mechanical stability of the deposited coating.[29] The PVA organic additive was used in the suspension preparation step to control the viscosity. During calcination, this additive decomposed and was removed from the coating, which leads to the deposited catalyst layer being more easily detached. This phenomenon was previously reported by Eleta et al.[29] when using polyvinyl alcohol in catalytic suspensions preparation.

Monolith surface areas presented no significant changes with respect to the uncoated aluminum substrate, being close to 40 $m^2 \cdot g_{monolith}^{-1}$. The pore radii reported in Table 3 for the coated monoliths correspond to those obtained from the pore size distributions, which proved to be bimodal (Figure 2). The first number corresponds to the substrate pore radius (bare anodized aluminum monolith, with an average pore radius of 1.87 nm) while the second number is attributed to the catalytic coating CS-30 (with a pore radius of 6.37 nm). The pore size distribution of the samples is shown in Figure 2, and the mentioned contributions are indicated with arrows.

An increase in the average pore radius of CS-30 compared to that of NiNbO catalyst was also observed. In the case of pore size distribution, CS-30 exhibited a decrease in the amount of pores with smaller diameter compared to NiNbO, which could be explained by the fact that that the silica particles added to the medium filled the smaller pores. This would be associated with the decrease in surface area. On the other hand, there was an increase in the amount of pores with a radius of 6–15 nm. These phenomena were previously reported for suspensions containing silica. Eleta et al.[29] observed that some mesoporosity was generated (with a pore diameter of about 10 nm) when silica was added to catalyst particles suspensions. They reported that the mesoporosity belongs neither to colloidal silica nor to the catalyst alone, and it is probably created during the drying and calcination process, when some hollows were formed in between the catalyst crystals, cemented by the silica particles. It was also observed that the final coating presents a drop in the amount of smaller radius pores and there was a decrease in specific surface area. Despite the loss of the small pores in the CS-30 sample, the formation of mesoporosity could account for the slight increase in pore volume

Table 3. Catalytic loading, adherence, and textural properties of the monolithic and powder samples

Sample	Coating silica:catalyst ratio (g/g)	Monolith catalyst load (mg)	Coatings	Adherence (%)	Surface area ($m^2 \cdot g_{monolith}^{-1}$)	Pore radius (nm)
MA15	0.23	178	9	99	39	1.92, 6.33
MA30	0.11	225	2	61	46	1.93, 4.85
MA30noPVA	0.11	276	3	86	43	1.92, 6.29
Uncoated substrate	–	–	–	–	41	1.87
CS-30	0.11	–	–	–	61[a]	6.37
NiNbO	–	–	–	–	81[a]	4.36

a) Specific surface area in $m^2 \cdot g_{catalyst}^{-1}$

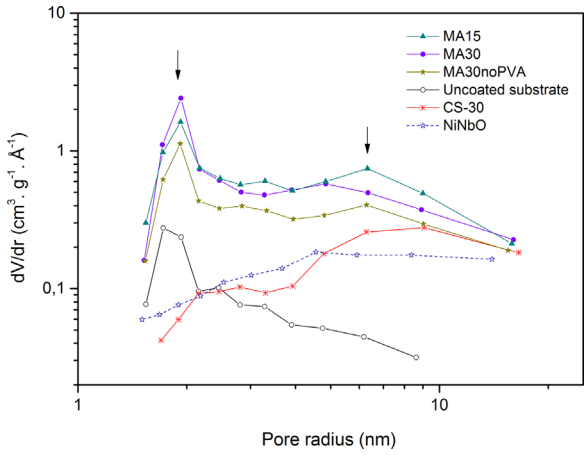

Figure 2. Pore size distribution of the studied samples.

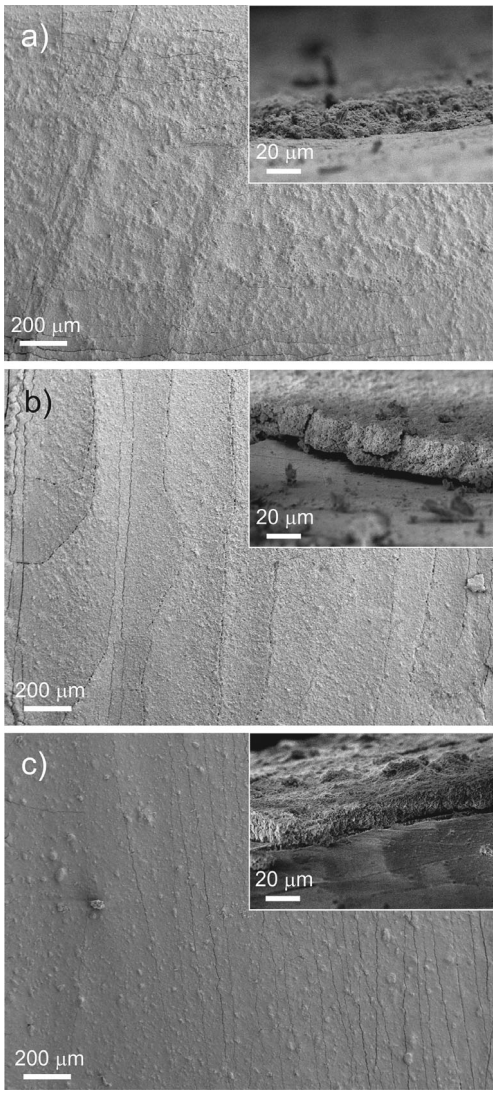

Figure 3. SEM images of the monolith surface after the coating procedure. (a) MA15, (b) MA30, and (c) MA30noPVA. The cross-sections of the catalytic layers are shown in the corresponding insets.

compared to NiNbO (0.195 $cm^3 \cdot g^{-1}$ for CS-30 and 0.182 $cm^3 \cdot g^{-1}$ for the catalyst).

Regarding the morphology of the deposited coatings, the surface of the monoliths was homogeneous, with a coating thickness between 5×10^{-6} and 18×10^{-6} m. The measured thickness refers to the Ni-Nb-O catalyst deposited on the aluminum monoliths after the anodizing process. It was only considered the catalytic material, excluding the alumina layer. The micrographs of the surface of the structured catalysts and cross-section of the deposited layers are shown in Figure 3.

Catalytic Tests

The monoliths coated with the Ni-Nb mixed oxides were tested for the ODH of ethane to obtain ethylene. The ethane conversion levels obtained for the structured catalysts and the CS-30 and NiNbO samples are shown in Figure 4. The samples exhibited activity at relatively low temperatures, in the 300–400 °C range.

The NiNbO catalyst presented the highest level of ethane conversion, reaching 57 % at 400 °C, which is similar to the conversion levels reported by Heracleous and Lemonidou.[17] The activity of the structured catalysts and the CS-30 sample was markedly lower. In order to make a better comparison of the catalytic performances, the powder samples specific surface activity (SSA) for ethane consumption at 350 °C was determined. It was observed that NiNbO exhibited a higher surface reactivity for ethane activation than the CS-30 sample (1.3×10^{-8} $mol_{C2H6} \cdot m^{-2} \cdot s^{-1}$ and 1.4×10^{-9} $mol_{C2H6} \cdot m^{-2} \cdot s^{-1}$, respectively). SSA values were determined under kinetic control.[24] The determination of the external diffusion limitations absence at each temperature was performed by varying the flow rate of gaseous reagents fed to the system, maintaining a constant W:F ratio and particle size. Internal mass transfer resistances were evaluated using the Weisz-Prater criterion,[30] and the absence of internal diffusional limitations was also observed under the selected operating conditions. In this way, the important difference in activity could be attributed to the presence of silica in the coatings, as will be discussed below in the section Analysis of the Effect of the Addition of Silica.

The structured catalysts presented similar conversion levels at each temperature studied. After the loss of activity observed for the lower silica:catalyst ratio monolith, a further increase in the silica concentration had no significant effect on conversion levels. For the catalytic tests, the experimental error on ethane conversion was estimated to be 10 %. The experimental uncertainty was

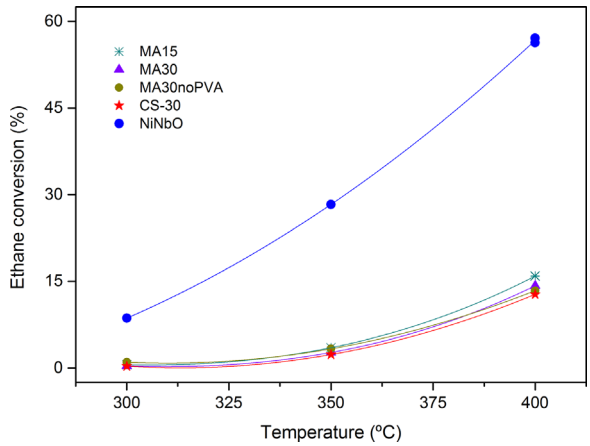

Figure 4. Ethane conversion at different reaction temperatures (operating conditions: $O_2/C_2H_6/N_2 = 5/5/90$, $W/F = 0.54$ g · s · cm^{-3}).

Table 4. Ethylene yields, product selectivities, and the corresponding ethane conversions at 350 and 400 °C for the different catalysts studied

	S_{C2H4} (%)		S_{CO2} (%)		X_{C2H6} (%)		Y_{C2H4} (%)	
	350 °C	400 °C	350 °C	400 °C	350 °C	400 °C	350 °C	400 °C
MA15	84.4	76.0	15.6	24.0	3.5	15.9	3.0	12.1
MA30	81.4	75.8	18.6	24.2	2.7	14.2	2.2	10.8
MA30noPVA	85.4	76.8	14.6	23.2	1.0	13.4	0.9	10.3
CS-30	83.5	76.3	16.5	23.7	2.3	13.7	1.9	10.5
NiNbO	81.8	72.3	18.2	27.7	28.3	56.7	23.1	41.0
NiNbO (W:F = 0.06 g · s · cm^{-3})	–	74.4	–	25.6	–	13.6	–	10.1

assessed by calculating the Percent Difference (see Experimental section). Differences in ethane conversion for the structured catalysts were within measurement error. An analogous behaviour was observed previously for structured catalysts prepared using the same inorganic binder with a different substrate material.[26]

The selectivities toward ethylene for the structured catalysts, the powder samples, and the uncoated substrate at 350 and 400 °C are presented in Table 4. The only carbon-containing reaction products obtained were ethylene and carbon dioxide, as previously reported in the literature.[17]

A high selectivity towards the olefin was observed, with no significant variations between values presented by the different samples at each temperature. In order to evaluate the influence of silica on the distribution of products under comparable conditions, an additional reaction experience was carried out. The NiNbO catalyst was tested with sufficiently low residence times (W: F = 0.06 g · s · cm^{-3}) to match the conversion levels of silica-containing samples. According to the data presented in Table 4, the presence of SiO_2 particles did not cause a notable change in the distribution of the reaction products. The presence of the substrate (anodized aluminum) on the selectivity towards ethylene was also negligible. It is known that alumina favours the oxidation of ethane to CO_2 and the dehydrogenation to coke. Both reactions take place on the OH acid groups and the Al^{3+}-O^{2-} acid sites.[31] However, under the operating conditions selected for the experiments, the selectivity towards ethylene was not significantly affected. Reaction tests with the uncoated aluminum substrate at maximum operating temperature (400 °C) resulted in ethane conversion levels lower than 0.4 %, thus generating small amounts of CO_2. This could be the reason why the powder catalyst CS-30 presented the same selectivity than the structured catalysts.

Analysis of the Effect of the Addition of Silica

In order to explain the effect of the addition of silica on catalyst performance in the ethane ODH reaction, the surface compositions, reducibility, and the phases present in the catalysts were analyzed. NiNbO and CS-30 powder samples were considered for the study. The surface compositions of the catalysts and of the reference compound SiO_2 are presented in Table 5.

Table 5. Surface atomic composition of the analyzed samples (%)

Element	NiNbO	CS-30	SiO_2
Nb	3.4	2.1	–
Ni	32.7	12.7	–
Si	–	22.1	35.2
O	63.9	63.1	64.8
Ni:Nb ratio	9.6	6.0	–

As expected, the concentration of Ni and Nb decreased in the CS-30 sample compared to those observed for NiNbO, due to the addition of silica. However, the decrease in the amount of surface Ni was more marked than that observed for Nb, as indicated by the lower Ni:Nb ratio in CS-30. Taking into account that nickel sites are associated with the activation of ethane,[17] the lower availability of this element could be the reason for the activity loss of CS-30. On the other hand, in the XPS spectrum of the CS-30 sample, a 0.6–0.7 eV (9 613 × 10^{-20} –1 122 × 10^{-19} J) shift was observed in the main line of $Ni2p_{3/2}$ region towards higher binding energies (Figure 5). This shift could be assigned to a weak interaction between silica particles and the catalyst surface. This difference in binding energy was observed at a similar magnitude, i.e. 0.8 eV (1 282 × 10^{-19} J), for a SiO_2-supported nickel oxide system.[32] In the Nb 3d region of the spectrum, the shift was less pronounced, with an increase in the binding energies of 0.2 eV (3204 × 10^{-20} J).

The surface oxygen concentration was very similar for the reference compounds NiNbO and SiO_2, and the CS-30 mixture presented virtually the same concentration (Table 5).

The XRD analysis of the samples indicated that the interaction between the nickel and silica species did not lead to the formation of new crystalline phases, at least within the detection limits of this technique. As shown in Figure 6, the contribution of the phases present in the NiNbO catalyst can be also observed in the diffractogram of the CS-30 sample, i.e. the peaks corresponding to NiO and $NiNb_2O_6$. A barely detectable increase in intensity was observed in the 2θ region between 15 and 30° for the CS-30 sample due to the presence of the amorphous silica particles.

The TPR profiles of the NiNbO pure catalyst and of the silica-containing CS-30 mixture are shown in Figure 7. A marked increase in the reduction temperature of CS-30 compared to NiNbO was observed. In the calcined suspension, the presence of silica particles covering the catalyst surface probably hinders the reduction process, producing a shift of 100 °C in the maximum H_2 consumption peak towards higher temperatures. A relationship between the reducibility of Ni-Nb mixed oxides and their activity in the ODH of ethane was reported in the literature.[23] In samples that are less easily reduced, the first step in the ODH of ethane (reduction of the catalyst surface) could be hindered. As this stage the limiting step of the reaction rate is considered. This could account for the lower activity observed for the CS-30 sample. In the case of the shoulder at 500 °C in the reduction of CS-30, it was reported for nickel oxide catalysts supported on SiO_2[33] that this signal could be attributed to the reduction of NiO, which has a close interaction with silica. It could also have a contribution of the Ni-O-Nb bonds reduction, corresponding to chemical species present in the pure nickel-niobium oxides, since this signal was previously observed for NiNbO catalysts.[24] For NiO-SiO_2 systems, which present a greater difficulty of reduction and a displacement of Ni binding energies in the XPS spectra, it has been reported that

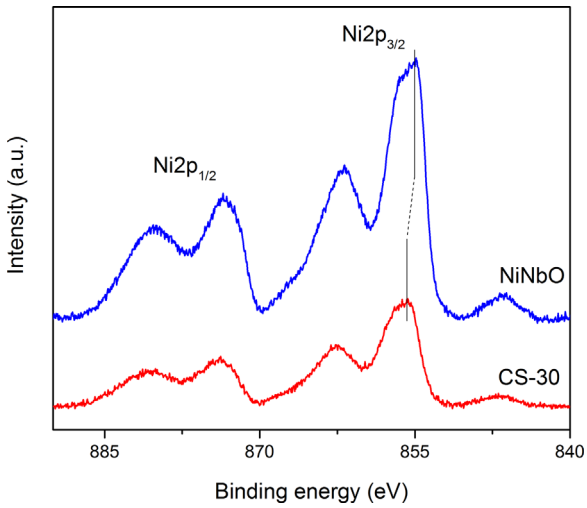

Figure 5. XPS spectra of the Ni 2p region for CS-30 and NiNbO samples.

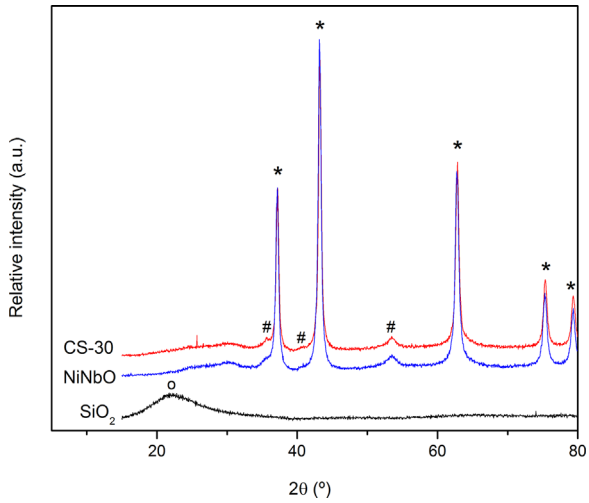

Figure 6. XRD patterns of NiNbO, CS-30 and SiO_2. (*) NiO, (#) $NiNb_2O_6$, (o) SiO_2.

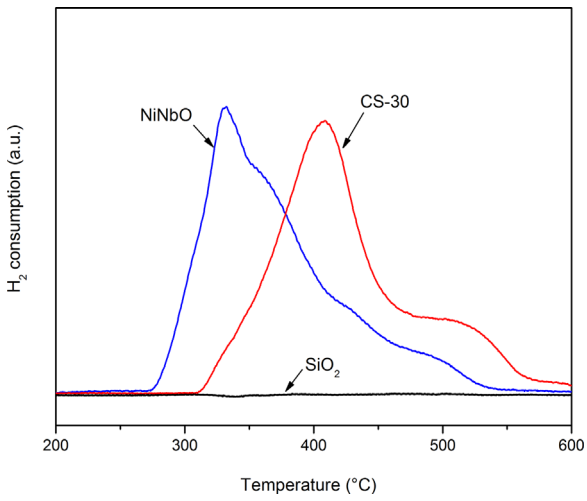

Figure 7. TPR profiles of the studied samples.

the interaction between the oxides could produce the electronic modification of the overall NiO particles, without the formation of a mixed compound at the NiO-SiO_2 interface.[34] These observations are in line with the results of the present work, where both a slight modification in the Ni oxidation state and an increase in the reduction temperature were observed.

Regarding the effect of silica particles on the specific area, a decrease of 25 % in surface area was observed for the CS-30 sample compared to the NiNbO catalyst (Table 2). However, the decrease in catalytic activity did not occur in the same proportion, where a drop of about 89 % was observed at 350 °C. This indicates that the loss of activity was not a result only of the decrease in specific area. The decrease in the amount of nickel exposed and the hindering of the reduction process would probably be the main causes of the loss of catalytic activity.

CONCLUSIONS

Anodized aluminum was used as substrate to support Ni-Nb mixed oxides, and coatings with good adherence, homogeneity, and the desired active phase load were obtained. Under reaction conditions this substrate did not produce significant changes in the catalytic performance of the mixed oxides in ethane ODH.

Enhanced levels of adherence were observed for the coatings with high silica/catalyst ratio, an effect mainly attributed to a better mechanical anchorage due to the accumulation of silica at the contact points between the catalyst particles.

Colloidal silica, an inorganic binder used to prepare suspensions for coating structured substrates, produced an important drop in the catalytic activity and ethylene yield in the ODH reaction over Ni-Nb mixed oxide catalysts.

The silica particles produced a preferential decrease in the concentration of surface nickel, and thus a decrease in the availability of nickel sites for the activation of ethane.

The lower activity could be also associated with the greater difficulty to reduce the silica-containing samples, given that the limiting step of the reaction rate in ethane ODH is the reduction of the catalytic surface.

Even though the use of silica produced homogeneous coatings with good adhesion to the structured substrates, the effect on the catalytic activity makes it necessary to explore the use of alternative inorganic binders that have a lower influence on the catalytic properties of the system.

ACKNOWLEDGEMENTS

The authors thank the Agencia Nacional de Promoción Científica y Tecnológica (National Agency of Scientific and Technological Promotion, Argentina) for the purchase of the Specs multitechnique analysis instrument (PME8-2003) and the Consejo Nacional de Investigaciones Científicas y Técnicas (National Council for Scientific and Technological Research) for the financial support.

NOMENCLATURE

SSA	specific surface activity (mol · m^{-2} · s^{-1})
S_{C2H4}	ethylene selectivity (%)
S_{CO2}	carbon dioxide selectivity (%)
X_{C2H6}	ethane conversion (%)
Y_{C2H4}	ethylene yield (%)

REFERENCES

[1] T. Ren, *Petrochemicals from Oil, Natural gas, Coal and Biomass: Energy Use, Economics and Innovation*, Ipskamp Drukkers B.V., Enschede **2009**.

[2] M. Neelis, M. Patel, K. Blok, W. Haije, P. Bach, *Energy* **2007**, *32*, 1104.

[3] F. Donsi, R. Pirone, G. Russo, *J. Catal.* **2002**, *209*, 51.

[4] M. Huff, L. D. Schmidt, *J. Phys. Chem.* **1993**, *97*, 11815.

[5] J. P. Bortolozzi, T. Weiss, L. B. Gutierrez, M. A. Ulla, *Chem. Eng. J.* **2014**, *246*, 343.

[6] R. M. Heck, S. Gulati, R. J. Farrauto, *Chem. Eng. J.* **2001**, *82*, 149.

[7] P. Avila, M. Montes, E. E. Miró, *Chem. Eng. J.* **2005**, *109*, 11.

[8] G. Kolb, V. Hessel, *Chem. Eng. J.* **2004**, *98*, 1.

[9] O. Sanz, F. Echave, J. Odriozola, M. Montes, *Ind. Eng. Chem. Res.* **2011**, *50*, 2117.

[10] N. Burgos, M. Paulis, A. Gil, L. M. Gandia, M. Montes, *Stud. Surf. Sci. Catal.* **2000**, *130*, 593.

[11] J. C. Ganley, K. L. Riechmann, E. G. Seebauer, R. I. Masel, *J. Catal.* **2004**, *227*, 26.

[12] D. Quattrini, D. Serrano, S. Perez Catán, *Granul. Matter* **2001**, *3*, 125.

[13] S. Lee, A. Gavriilidis, *Catal. Commun.* **2002**, *3*, 425.

[14] O. Sanz, L. M. Martínez T, F. J. Echave, M. I. Domínguez, M. A. Centeno, J. A. Odriozola, M. Montes, *Chem. Eng. J.* **2009**, *151*, 324.

[15] O. Sanz, L. C. Almeida, J. M. Zamaro, M. A. Ulla, E. E. Miró, M. Montes, *Appl. Catal. B-Environ.* **2008**, *78*, 166.

[16] H. Feng, J. W. Elam, J. A. Libera, M. J. Pellin, P. C. Stair, *Chem. Eng. Sci.* **2009**, *64*, 560.

[17] E. Heracleous, A. A. Lemonidou, *J. Catal.* **2006**, *237*, 162.

[18] H. Zhu, H. Dong, P. Laveille, Y. Saih, V. Caps, J. Basset, *Catal. Today* **2014**, *228*, 58.

[19] B. Solsona, P. Concepción, B. Demicol, S. Hernández, J. J. Delgado, J. J. Calvino, J. M. López Nieto, *J. Catal.* **2012**, *295*, 104.

[20] Z. Skoufa, G. Xantri, E. Heracleous, A. A. Lemonidou, *Appl. Catal. A-Gen.* **2014**, *471*, 107.

[21] E. Heracleous, A. A. Lemonidou, *J. Catal.* **2010**, *270*, 67.

[22] B. Savova, S. Loridant, D. Filkova, J. M. M. Millet, *Appl. Catal. A-Gen.* **2010**, *390*, 148.

[23] H. Zhu, S. Ould-Chikh, D. H. Anjum, M. Sun, G. Biausque, J. Basset, V. Caps, *J. Catal.* **2012**, *285*, 292.

[24] J. A. Santander, E. López, A. Diez, M. Dennehy, M. N. Pedernera, G. M. Tonetto, *Chem. Eng. J.* **2014**, *255*, 185.

[25] J. F. Sánchez M, D. E. Boldrini, G. M. Tonetto, D. E. Damiani, *Chem. Eng. J.* **2011**, *167*, 355.

[26] J. A. Santander, E. López, G. M. Tonetto, M. N. Pedernera, *Ind. Eng. Chem. Res.* **2014**, *53*, 11312.

[27] G. Tonetto, D. Damiani, *J. Mol. Catal.* **2003**, *202*, 289.

[28] T. A. Nijhuis, A. E. W. Beers, T. Vergunst, I. Hoek, F. Kapteijn, J. A. Moulijn, *Catal. Rev.* **2001**, *43*, 345.

[29] A. Eleta, P. Navarro, L. Costa, M. Montes, *Micropor. Mesopor. Mat.* **2009**, *123*, 113.

[30] H. S. Fogler, *Elements of chemical reaction engineering*, 3rd edition, Prentice Hall, Upper Saddle River **1999**.

[31] E. Heracleous, A. A. Lemonidou, *Catal. Today* **2006**, *112*, 23.

[32] Y. Liu, J. Chen, J. Zhang, *Chinese J. Chem. Eng.* **2007**, *15*, 63.

[33] A. M. Diskin, R. H. Cunningham, R. M. Ormerod, *Catal. Today* **1998**, *46*, 147.

[34] J. P. Bonnelle, B. Delmon, E. Derouane, *Surface Properties and Catalysis by Non-Metals*, D. Reidel Publishing Company, Dordrecht **1983**.

Manuscript received July 24, 2016; revised manuscript received January 10, 2017; accepted for publication January 11, 2017.